DALTON
FULL PAPER

Peripherally-metallated porphyrins: preparations, spectroscopic properties and structural studies of *trans*-[PtBr(MDPP)(PPh_3)$_2$] (DPP = dianion of 5,15-diphenylporphyrin, M = MnCl, Co, Ni, Zn) and related *meso*-η^1-organoplatinum porphyrins †

Margaret J. Hodgson,[a] Peter C. Healy,*[b] Michael L. Williams[b] and Dennis P. Arnold*[a]

[a] *Centre for Instrumental and Developmental Chemistry, School of Physical and Chemical Sciences, Queensland University of Technology, G.P.O. Box 2434, Brisbane 4001, Australia*
[b] *School of Science, Griffith University, Nathan 4111, Australia*

Received 3rd May 2002, Accepted 1st October 2002
First published as an Advance Article on the web 4th November 2002

A series of *meso*-η^1-platiniometalloporphyrins comprising DPP (= dianion of 5,15-diphenylporphyrin) and the first row transition metal ions Mn(III), Co(II), Ni(II) and Zn(II) has been prepared. The syntheses, spectroscopy and voltammetry as well as crystal structures of several of these derivatives are reported. The –PtBr(PPh_3)$_2$ moiety attached to the macrocycle at the *meso* position is a strong electron donor, as shown by its effects on spectra, oxidation potentials and reactivity. The crystal structures of *trans*-[PtBr(MDPP)(PPh_3)$_2$]·0.5CH_2Cl_2, where M = Co (**16**), Ni (**14**) and Zn (**17**), and *trans*-[PtBr(NiDPPBr)(PPh_3)$_2$] were determined. The structures exhibit non-planar distortions of the macrocycle which are best described as hybrids of typical ruffled and saddled conformations.

Introduction

The chemistry of porphyrins directly bonded to a metal ion through a peripheral carbon-to-metal σ-bond is very undeveloped at present. Most representatives of "organometallic" porphyrins comprise those with hydrocarbyl ligands bound to a metal ion which is coordinated to the pyrrolic nitrogens. This field has been thoroughly reviewed recently.[1] Of other possible types of organometallic porphyrins, there exist examples in which the metal is bonded in either σ or π fashion to a peripheral aryl substituent[2] or η^5-bound to a pyrrole ring[3] (or to the fused benzo ring of a phthalocyanine[4]), and there has been much recent interest in the porphyrinoid macrocycles with the N_3C core—"inverted" or "N-confused" porphyrins[5] and carbaporphyrins[6] and their complexes. This last class includes examples in which the central metal ion is coordinated to three pyrrole nitrogens and one carbon of the inverted ring (or in one recent case, to two carbons of a doubly N-confused macrocycle).

Our interest in η^1-*meso*-metalloporphyrins arose from our work on Pd-catalysed couplings involving *meso*-bromoporphyrins, especially derivatives of 5,15-diphenylporphyrin (H_2DPP, **1**).[7] We isolated and characterised by X-ray crystallography the first example of a *meso*-η^1-palladioporphyrin[8] and subsequently expanded this work to include a variety of *meso*-palladio- and platinio-porphyrins.[9] Amongst other examples of peripherally-metallated porphyrins, there are the *meso*-boronated DPP derivatives prepared by the Therien group,[10] various phosphonium[11] and arsonium salts,[12] and the mercury(II) derivatives prepared by the Smith group.[13]

So far, we have reported a range of DPP complexes containing the fragments –PdBrL_2 and –PtBrL_2, where L = PPh_3, and –PdBr(L–L) where L–L = dppe, dppp and dppf.[8,9] The X-ray crystal structures of three of these complexes have been reported, namely [PdBr(H_2DPP)(dppe)],[8] *trans*-[PtBr(H_2DPP)(PPh_3)$_2$]·0.25CH_2Cl_2 and *cis*-[PtBr(NiDPP)(PPh_3)$_2$].[9] A common feature revealed by crystal structures and NMR spectra is the significant occlusion of the face of the porphyrin by at least one of the phenyl groups of the phosphine ligand(s). This fact suggested that these substituents may be useful as moieties for the facile construction of molecules with a controllable degree of steric encumbrance above and below the porphyrin plane. In view of the apparent high stability of these compounds, they may be useful as catalysts using the metal ion in the centre of the porphyrin as a catalytically-active site, and the superstructure provided by the phosphines as a shape-selective region. By the use of chiral chelating diphosphines, the molecules may also be useful for chiral recognition of ligands coordinated to the metalloporphyrin. This requires us to be able to vary the metal ion in the central cavity and include those which are known to act as biomimetic oxidation and dehalogenation catalysts, *e.g.* Mn, Fe, Co *etc*. We have therefore extended our range of organoplatinum derivatives to include first row metal ions other than Ni(II), namely Mn(III), Co(II) and Zn(II). In this paper we report the results of our synthetic and electrochemical work as well as crystal structures of a number of these derivatives. These studies have allowed us to investigate the electronic and steric effects of the –PtX(PPh_3)$_2$ moiety attached to the DPP macrocycle, and will guide us in designing new molecules based on this novel *meso*-metalloporphyrin structural motif.

Experimental

General

Instruments, solvents and general procedures were as described in our previous publication.[9] UV–visible spectra were recorded in CH_2Cl_2. ^{1}H NMR spectra were recorded at 300 MHz in $CDCl_3$, referenced to the solvent residual peak at 7.26 ppm, and ^{31}P spectra at 121.4 MHz in $CDCl_3$, referenced to external 85% H_3PO_4. For the electrochemical measurements, a standard three-electrode configuration was used, with Pt button working electrode and a Pt wire counter electrode. The reference electrode comprised a silver wire coated with silver chloride

† Electronic supplementary information (ESI) available: linear displays of the deviations of the macrocycle atoms from the $C_{20}N_4$ least-squares plane for complexes **14**, **16** and **17** (this work) and free base **12** (from ref. 9). See http://www.rsc.org/suppdata/dt/b2/b205295b/

Table 1 Correspondence of compound numbers and structures

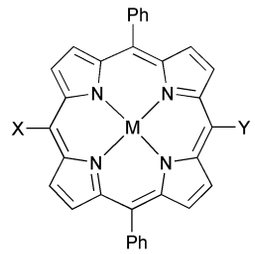

Compound	M	X	Y
1	H_2	H	H
2	H_2	H	Br
3	H_2	Br	Br
4	MnCl	H	H
5	Co	H	H
6	Ni	H	H
7	MnCl	H	Br
8	Co	H	Br
9	Ni	H	Br
10	Zn	H	Br
11	H_2	H	*cis*-PtBr(PPh_3)$_2$
12	H_2	H	*trans*-PtBr(PPh_3)$_2$
13	MnCl	H	*trans*-PtBr(PPh_3)$_2$
14	Co	H	*trans*-PtBr(PPh_3)$_2$
15	Ni	H	*cis*-PtBr(PPh_3)$_2$
16	Ni	H	*trans*-PtBr(PPh_3)$_2$
17	Zn	H	*trans*-PtBr(PPh_3)$_2$
18	Ni	Br	Br
19	Ni	Br	*trans*-PtBr(PPh_3)$_2$
20	Ni	*trans*-PtBr(PPh_3)$_2$	*trans*-PtBr(PPh_3)$_2$
21	Ni	*trans*-PtBr(PPh_3)$_2$	*trans*-PdBr(PPh_3)$_2$
22	H_2	H	*trans*-PdBr(PPh_3)$_2$
23	Ni	H	*trans*-PdBr(PPh_3)$_2$

separated from the working solution by two fritted jackets. The internal chamber containing the wire was filled with 0.05 M Bu_4NCl–0.45 M Bu_4NPF_6, and the external chamber contacting the working solution was filled with 0.5 M Bu_4NPF_6, all in CH_2Cl_2. The working solution was pre-purged and subsequently protected with N_2. The voltammetry was carried out at The Research School of Chemistry, The Australian National University, in CH_2Cl_2 (freshly distilled from CaH_2 under N_2) containing 0.5 M Bu_4NPF_6, using a PAR model 170 system linked to an Apple Macintosh LC630 computer *via* a Maclab interface controlled by EChem software (AD Instruments). Electrode potentials are reported using ferrocene as internal standard [E^0(ox) = +0.55 V]. The stated E^0 values were operationally defined by the ac peak potentials (or the mean of the forward and reverse ac peak potentials in some cases where these were not precisely coincident).

Porphyrin starting materials H_2DPP **1**,[14] H_2DPPBr **2**[14,15] and H_2DPPBr$_2$ **3**[14,15] and the complexes NiDPPBr **9**, NiDPPBr$_2$ **18**[7] and ZnDPPBr **10**[14] were prepared by literature procedures, as was Pt(PPh_3)$_3$.[16] The free-base organometallic porphyrin *trans*-[PtBr(H_2DPP)(PPh_3)$_2$] **12** was available from our previous work.[9] Metal salts were commercial analytical reagent quality. Crystals for X-ray structure determinations were grown as thin plates or needles by slow diffusion of hexane into a CH_2Cl_2 solution of the complex. A list of the complexes is given in Table 1.

Metallation of H_2DPP

Chloro(5,15-diphenylporphyrinato)manganese(III) 4. To a solution of H_2DPP (23 mg, 0.05 mmol) in $CHCl_3$ (10 mL) were added 2,6-lutidine (2 drops) and $MnCl_2$·$4H_2O$ (158 mg, 0.8 mmol) in methanol (2 mL). After refluxing for 2.5 h, the solution was washed with water to remove excess metal salt. After drying the organic solution with $MgSO_4$, the solvent was removed to leave a dark green residue, which was recrystallised from CH_2Cl_2–hexane to give a dark green–purple powder (21 mg, 70%) (Found: C, 67.92; H, 3.86; N, 9.67. $C_{32}H_{20}ClMnN_4$·$0.5CH_2Cl_2$ requires C, 68.14; H, 3.64; N, 9.63%); λ_{max}/nm 347 (sh) (ε/10^3 dm^3 mol^{-1} cm^{-1} 41.5), 367 (53.9), 392 (33.5), 442 (10.2), 470 (94.0), 518 (4.4), 568 (9.0), 599 (5.3), 679 (vbr) (0.7), 750 (0.8); δ_H −25 (4H, vbr, βH), −22 (4H, vbr, βH), 8.4 (vbr, overlapping signals for 5,15-Ph), 45 (vbr, *meso*-H); *m*/*z* (FAB) 515.0 (M − Cl).

(5,15-Diphenylporphyrinato)cobalt(II) 5. To a solution of H_2DPP (23 mg, 0.05 mmol) in $CHCl_3$ (20 mL) containing triethylamine (1 mL) was added a solution of Co(OAc)$_2$·$4H_2O$ (187 mg, 0.75 mmol) in methanol (4 mL), and the mixture was refluxed for 2.5 h. The solvents were removed by rotary evaporation and the residue was dissolved in CH_2Cl_2, the solution was washed with water to remove excess salt, then dried with $MgSO_4$ and concentrated to a dark red residue which was recrystallised from CH_2Cl_2–hexane to give a fine orange–purple powder. The preparation of this compound from Co(acac)$_2$ was previously reported by Shelnutt and co-workers.[17] λ_{max}/nm 401 (ε/10^3 dm^3 mol^{-1} cm^{-1} 267), 516 (13.7), 543 (sh) (5.6); δ_H 9.5 (2H, *p*-H of 5,15-Ph), 9.7 (4H, *m*-H of 5,15-Ph), 12.4 (4H, br, *o*-H of 5,15-Ph), 15.2, 17.2 (each 4H, br, βH), 24.1 (vbr, *meso*-H); *m*/*z* (FAB) 519.1 (M^+).

Metallation of H_2DPPBr

Chloro(5-bromo-10,20-diphenylporphyrinato)manganese(III) 7. This complex was prepared as described above for **4**, from H_2DPPBr (27 mg, 0.05 mmol), yielding the product as fine dark green–purple crystals (28 mg, 88%). (Found: C, 60.68; H, 3.10; N, 8.89. $C_{32}H_{19}BrClMnN_4$ requires C, 61.02; H, 3.04; N, 8.90%); λ_{max}/nm 332 (sh) (ε/10^3 dm^3 mol^{-1} cm^{-1} 32.9), 348 (49.5), 374 (62.5), 400 (50.6), 478 (113), 529 (5.4), 582 (9.7), 617 (9.1), 693 (vbr) (0.5), 763 (0.5); ^{1}H NMR data were unobtainable due to poor solubility and very broad peaks; *m*/*z* (FAB) 593.9 (M − Cl).

(5-Bromo-10,20-diphenylporphyrinato)cobalt(II) 8. This complex was prepared as described above for **5**, from H_2DPPBr (27 mg, 0.05 mmol), yielding the product as fine orange–purple crystals (18 mg, 53%) (Found: C, 59.07; H, 3.24; N, 8.47. $C_{32}H_{19}BrCoN_4$·CH_2Cl_2 requires C, 58.73; H, 3.04; N, 8.06%); λ_{max}/nm 407 (ε/10^3 dm^3 mol^{-1} cm^{-1} 247), 525 (13.7); δ_H 9.59 (2H, *p*-H of 10,20-Ph), 9.77 (4H, *m*-H of 10,20-Ph), 12.6 (4H, br, *o*-H of 10,20-Ph), 15.0, 15.6, 16.5, 17.1 (each 2H, br, βH), 27 (vbr, *meso*-H); *m*/*z* (FAB) 597.0 (M^+).

Preparation of *trans*-Pt(PPh_3)$_2$Br adducts

***trans*-[PtBr(MnClDPP)(PPh_3)$_2$] 13.** (a) Toluene (5 mL) was placed in a Schlenk flask and heated to 105 °C under a stream of Ar. Pt(PPh_3)$_3$ (11.8 mg, 0.012 mmol) was added, followed by MnCl(DPPBr) (6.3 mg, 0.01 mmol). The Mn porphyrin dissolved slowly over an hour. The reaction mixture was stirred under Ar at 105 °C for 5 h, then cooled, and the solvent was removed under vacuum. The residue was washed with hexane (3 mL) and then recrystallised from CH_2Cl_2–hexane to give **13** as dark green crystals (8.6 mg, 64%) (Found: C, 60.05; H, 3.78; N, 4.12. $C_{68}H_{49}BrClMnN_4P_2Pt$ requires C, 60.52; H, 3.66; N, 4.15%); λ_{max}/nm 345 (sh) (ε/10^3 dm^3 mol^{-1} cm^{-1} 25.9), 361 (sh) (29.7), 386 (35.0), 410 (34.0), 426 (30.8), 484 (71.0), 541 (4.5), 603 (7.0), 635 (10.0); δ_H −31 (4H, vbr, βH), −22 (2H, vbr, βH), −17 (2H, vbr, βH), *ca.* 8.4 (vbr, overlapping signals for 10,20-Ph), 3–15 (vbr, including peak at *ca.* 7, P-phenyl groups), 47 (vbr, *meso*-H); δ_P −26, 68 [pair of br d, ^2J(PP) 420 Hz, ^1J(PtP) see text and Fig. 1]; *m*/*z* (FAB) 1349.1 (M^+, 13%), 1313.1 (M − HCl, 100%). (b) This complex was also prepared as follows. To a solution of *trans*-[PtBr(H_2DPP)(PPh_3)$_2$] (25 mg, 0.02 mmol) in $CHCl_3$ (10 mL) were added 2,6-lutidine (2 drops) and

$MnCl_2·4H_2O$ (63 mg, 0.32 mmol) in methanol (2 mL). After refluxing for 9 h, the solution was washed with water to remove excess metal salt. After drying the organic solution with $MgSO_4$, the solvent was removed to leave a dark green residue, which was recrystallised from CH_2Cl_2–hexane to give a dark green crystalline material (17.5 mg, 65%).

***trans*-[PtBr(CoDPP)(PPh$_3$)$_2$] 14.** (a) Toluene (5 mL) was placed in a Schlenk flask and heated to 105 °C under a stream of Ar. $Pt(PPh_3)_3$ (11.8 mg, 0.012 mmol) was added, followed by Co(DPPBr) (6 mg, 0.01 mmol). The mixture was stirred under Ar at 105 °C for 6 h, after which it was cooled, and the solvent was removed under vacuum. The residue was subjected to chromatography through a short column of silica gel, eluting with CH_2Cl_2–hexane–triethylamine 70:30:1 (v/v). Traces of unreacted CoDPPBr eluted first, followed by the main product, and then a weak band due to the corresponding *cis* isomer. The *trans* isomer was recrystallised from CH_2Cl_2–hexane to give dark purple crystals (8.3 mg, 63%) (Found: C, 60.73; H, 3.71; N, 4.06. $C_{68}H_{49}BrCoN_4P_2Pt·0.5CH_2Cl_2$ requires C, 60.65; H, 3.69; N, 4.10%); λ_{max}/nm 420 (ε/103 dm^3 mol^{-1} cm^{-1} 214), 533 (12.4), 567 (sh) (4.2); δ_H −2.2 (vbr, PPh), 1.5 (vbr, PPh), 5.6 (br, PPh), 9.55 (2H, *p*-H of 10,20-Ph), 9.70 (4H, *m*-H of 10,20-Ph), 12.6 (4H, br, *o*-H of 10,20-Ph), 15.5, 15.8, 17.1, 17.9 (each 2H, br, βH), 29.5 (vbr, *meso*-H); δ_P 24.1 [s, ^1J(PtP) 2965 Hz]; *m*/*z* (FAB) 1317.1 (M^+). (b) This complex was also prepared as follows. To a solution of *trans*-[PtBr(H_2DPP)(PPh_3)$_2$] (25 mg, 0.02 mmol) in $CHCl_3$ (20 mL) containing triethylamine (1 mL) was added a solution of $Co(OAc)_2·4H_2O$ (75 mg, 0.3 mmol) in methanol (4 mL), and the mixture was refluxed for 27 h. The solvents were removed by rotary evaporation and the residue was dissolved in CH_2Cl_2 and the solution was passed through a short column of silica gel to remove excess salt. The eluate was concentrated to a dark red residue which was recrystallised from CH_2Cl_2–hexane to give dark purple crystals (20 mg, 76%).

***trans*-[PtBr(NiDPP)(PPh$_3$)$_2$] 16.** (a) The preparation of this complex by oxidative addition of NiDPPBr to $Pt(PPh_3)_3$ was described previously.[8,9] (b) A solution of *trans*-[PtBr(H_2DPP)(PPh_3)$_2$] (12.6 mg, 0.01 mmol) and Ni(acac)$_2$ (12.8 mg, 0.05 mmol) in 1,2-dichloroethane (50 mL) and triethylamine (0.5 mL) was refluxed for 3.5 h. The volatiles were removed under vacuum, the residue was dissolved in CH_2Cl_2 and passed through a short column of silica gel, eluting with CH_2Cl_2. The isolated complex was recrystallised from CH_2Cl_2–hexane to give **16** as glistening purple plates (10 mg, 76%). Spectroscopic data were as reported previously.[8]

***trans*-[PtBr(ZnDPP)(PPh$_3$)$_2$] 17.** (a) This complex was prepared by method (a) as described above for **14**, and obtained as bright purple crystals (7.0 mg, 53%) (Found: C, 60.68; H, 3.74; N, 4.08. $C_{68}H_{49}BrN_4P_2PtZn·0.5CH_2Cl_2$ requires C, 60.35; H, 3.67; N, 4.08%); λ_{max}/nm 369 (ε/10^3 dm^3 mol^{-1} cm^{-1} 12.5), 430 (443), 482 (3.5), 518 (3.1), 555 (14.9), 599 (7.3); δ_H 6.35–6.50 (18H, m, PPh), 7.20–7.35 (m, PPh), 7.72 (6H, m, *m*-, *p*-H of 10,20-Ph), 8.13 (4H, m, *o*-H of 10,20-Ph), 8.50, 8.90, 9.19, 9.92 (each 2H, d, βH), 9.93 (^{1}H, s, *meso*-H); δ_P 23.5 [s, ^1J(PtP) 2989 Hz]; *m*/*z* (FAB) 1324.0 (M^+). (b) To a refluxing solution of *trans*-[PtBr(H_2DPP)(PPh_3)$_2$] (25 mg, 0.02 mmol) in $CHCl_3$ (20 mL) containing triethylamine (1 mL) was added a solution of $Zn(OAc)_2·2H_2O$ (22 mg, 0.1 mmol) in methanol (2 mL), and the mixture was refluxed for 27 h. After treatment as described above under 14 (b), the product was obtained as purple crystals (20 mg, 75%). When the triethylamine was omitted, the reaction was complete in less than 3 h, as shown by UV-visible spectroscopy.

{5-Bromo-15-[*trans*-PtBr(PPh$_3$)$_2$](NiDPPBr)} 19 and {5,15-bis[*trans*-PtBr(PPh$_3$)$_2$](NiDPP)} 20. Toluene (10 mL) was added to a Schlenk flask and heated to 105 °C under a stream of argon. $Pt(PPh_3)_3$ (98 mg, 0.10 mmol) was added, followed by $NiDPPBr_2$ 18 (27 mg, 0.04 mmol). The mixture was heated at 105 °C for 4 h. At this point, TLC analysis showed that no further change was occurring, so the solvent was removed under vacuum, and the residue was subjected to column chromatography on silica gel, eluting with CH_2Cl_2–hexane 70:30 (v/v). The mono-addition product **19** was eluted first, followed by **20**, and the complexes were recrystallised from CH_2Cl_2–hexane as bright purple crystals and fine dark purple needles, respectively. Data for **19**: (21 mg, 37%) (Found: C, 58.48; H, 3.46; N, 3.98. $C_{68}H_{48}Br_2N_4NiP_2Pt$ requires C, 58.48; H, 3.46; N, 4.01%); λ_{max}/nm 432 (ε/10^3 dm^3 mol^{-1} cm^{-1} 174), 545 (12.2), 579 (sh) (3.8); δ_H 6.55–6.75 (18H, m, PPh), 7.2–7.3 (m, PPh), 7.64 (6H, m, *m*-, *p*-H of 10,20-Ph), 7.86 (4H, m, *o*-H of 10,20-Ph), 8.12, 8.57, 9.29, 9.40 (each 2H, d, βH); δ_P 23.1 [s, ^1J(PtP) 2918 Hz]; *m*/*z* (FAB) 1396.0 (M^+). Data for **20**: (27 mg, 32%) (Found: C, 58.44; H, 3.72; N, 2.64. $C_{104}H_{78}Br_2N_4NiP_4Pt_2$ requires C, 59.02; H, 3.71; N, 2.65%); λ_{max}/nm 443 (ε/10^3 dm^3 mol^{-1} cm^{-1} 283), 507 (13.3), 551 (23.3), 594 (16.1); δ_H 6.7 (36H, m, PPh), 7.3 (m, PPh), 7.60 (6H, m, *m*-, *p*-H of 10,20-Ph), 7.85 (4H, m, *o*-H of 10,20-Ph), 8.07, 9.48 (each 4H, d, βH); δ_P 22.6 [s, ^1J(PtP) 2971 Hz]; *m*/*z* (FAB) 2116.5 (M^+).

X-Ray crystallography

Data collection, structure solution and refinement. Unique data sets were collected at 295 K for compounds **14**, **16**, **17** and **19** with a Rigaku AFC7R rotating anode diffractometer (ω–2θ scan mode, monochromated Mo-Kα radiation λ = 0.7107 Å) to $2\theta_{max}$ = 50°, yielding N independent reflections, N_o with $I > 2\sigma(I)$ being considered 'observed'. Empirical absorption correction was applied based on ψ-scans. The structures were solved by direct methods, expanded by using Fourier techniques and refined by full-matrix least squares on $|F|$ for observed data using the teXsan for Windows crystallographic software package, version 1.06, from the Molecular Structure Corporation.[18] Non-hydrogen atoms for all complexes except **16** were refined anisotropically. In **16**, marginal crystal quality yielded data sets that did not support anisotropic refinement of all of the carbon and nitrogen atoms and these were refined isotropically; (x,y,z,U_{iso})H were included and constrained at estimated values. Flack parameters for compounds **14** [0.0040(1)], **16** [0.0055(1)] and **17** [0.0002(1)] supported the proposed absolute structures. Conventional residues, R, R_w are quoted at convergence; weights derivative of $w = 1/[\sigma^2(F)]$ were employed.

Crystal data. 14. *trans*-[PtBr(CoDPP)(PPh_3)$_2$]·0.5CH_2Cl_2, $C_{68.5}H_{50}BrClCoN_4P_2Pt$, M = 1360.5, monoclinic, space group $P2_1$ (C_2^2, no. 4), a = 13.344(2), b = 29.730(6), c = 14.451(2) Å, β = 91.10(1)°, V = 5732(2) Å^3, Z = 4, D_c = 1.58 g cm^{-3}, μ = 35.7 cm^{-1}, crystal size: 0.50 × 0.35 × 0.10 mm; $T_{min,max}$ = 0.420, 0.703, N = 10316, N_o = 8123; R = 0.043 R_w = 0.040.

16. *trans*-[PtBr(NiDPP)(PPh_3)$_2$]·0.5CH_2Cl_2, $C_{68.5}H_{50}BrClN_4NiP_2Pt$, M = 1360.3, monoclinic, space group $P2_1$, a = 13.333(6), b = 29.719(4), c = 14.441(7) Å, β = 91.14(4)°, V = 5721(3) Å^3, Z = 4, D_c = 1.58 g cm^{-3}, μ = 36.1 cm^{-1}, crystal size: 0.45 × 0.25 × 0.12 mm; $T_{min,max}$ = 0.497, 0.652, N = 10343, N_o = 7465; R = 0.064 R_w = 0.068.

17. *trans*-[PtBr(ZnDPP)(PPh_3)$_2$]·0.5CH_2Cl_2, $C_{68.5}H_{50}BrClN_4P_2PtZn$, M = 1366.95, monoclinic, space group $P2_1$, a = 13.386(6), b = 29.890(7), c = 14.523(5) Å, β = 90.75(3)°, V = 5810(3) Å^3, Z = 4, D_c = 1.56 g cm^{-3}, μ = 36.4 cm^{-1}, crystal size = 0.60 × 0.20 × 0.15 mm; $T_{min,max}$ = 0.491, 0.583, N = 10225, N_o = 6730; R = 0.043 R_w = 0.042.

19. *trans*-[PtBr(NiDPPBr)(PPh_3)$_2$], $C_{68}H_{48}Br_2N_4NiP_2Pt$, M = 1396.70, triclinic, space group $P\bar{1}$ (C_i^1, no. 2), a = 14.252(6), b = 15.381(6), c = 13.474(5) Å, α = 105.86(3), β = 91.20(3), γ = 78.23(4)°, V = 2780(2) Å^3, Z = 2, D_c = 1.67 g cm^{-3}, μ = 43.9

cm^{-1}, crystal size: 0.60 × 0.30 × 0.05 mm; $T_{min,max}$ = 0.365, 0.817, N = 9777, N_o = 7165; R = 0.033 R_w = 0.032.

CCDC reference numbers 186868–186871.

See http://www.rsc.org/suppdata/dt/b2/b205295b/ for crystallographic data in CIF or other electronic format.

Results and discussion

Syntheses

We used the two strategies shown in Scheme 1 to obtain the

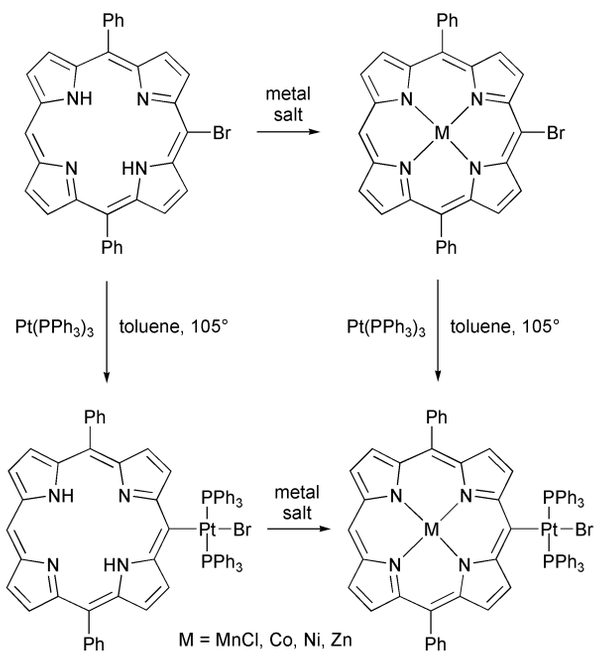

Scheme 1

series of complexes *trans*-[PtBr(MDPP)(PPh_3)$_2$]. The sequence H_2DPPBr ⟶ MDPPBr ⟶ *trans*-[PtBr(MDPP)(PPh_3)$_2$] involves metallation followed by oxidative addition to Pt(0), while the alternative involves the opposite order of reactions. It is by far preferable to use the latter sequence, since the complexes of DPPBr are rather insoluble (especially that of MnCl), and so are more difficult to handle than the common intermediate Pt free-base *trans*-[PtBr(H_2DPP)(PPh_3)$_2$] **12**. However, for the purposes of spectroscopic comparisons and completeness, we carried out both sequences on all four metal ions Mn(III), Co(II), Ni(II) and Zn(II). In addition, to assist in assigning the ^{1}H NMR spectra of the complexes of the paramagnetic Mn and Co ions, we also prepared their complexes with H_2DPP, namely **4** and **5**, respectively. To our knowledge, the complexes MnCl(DPP) **4** and MnCl(DPPBr) **7** have not been previously reported. We used the method of Borovkov *et al.* to insert Mn(III),[19] using $MnCl_2$ in the presence of 2,6-lutidine as base, but as for all complexes of the DPP ligand, metal insertion is much slower than for octaalkylporphyrins. CoDPP **5** was reported by Shelnutt and co-workers,[17] but CoDPPBr **8** is new, and the electronic spectral data for **5** have not previously been reported. The analogous Ni complex **9** and Zn complex **10** were first reported by ourselves[7] and Therien and co-workers, respectively.[14]

Conversion of the MDPPBr metalloporphyrins into the respective *trans*-[PtBr(MDPP)(PPh_3)$_2$] complexes was achieved by oxidative addition to the Pt(0) precursor Pt(PPh_3)$_3$ under our standard conditions of heating in near-boiling toluene. The reactions were continued long enough for the initially-formed *cis* adducts to be converted to the *trans* complexes (*ca.* 6 h). In our previous work, we showed how the *cis* adducts [PtBr(H_2DPP)(PPh_3)$_2$] **11** and [PtBr(NiDPP)(PPh_3)$_2$] **15** could be isolated by interrupting the reaction after partial conversion of the bromo starting material.[9] Purification of *trans*-[PtBr(CoDPP)(PPh_3)$_2$] **14** and *trans*-[PtBr(ZnDPP)(PPh_3)$_2$] **17** was achieved by column chromatography, but the analogous MnCl complex **13** was immobile on silica gel in weakly polar solvents, presumably due to binding of active sites to the axial position, so recrystallisation was used for purification.

For the alternative route to the complexes containing the *trans*-PtBr(PPh_3)$_2$ moiety, namely metallation of the free-base *trans*-[PtBr(H_2DPP)(PPh_3)$_2$], the same metallation methods as for MDPPBr were employed. We took the precaution in these reactions of adding excess triethylamine as an acid scavenger in the case the Pt–C bond was labile under metallation conditions. The metallations of this unusual porphyrin free base are unexpectedly rather slow under these conditions. In fact, completion of Zn(II) insertion required over 24 h, a very long time for such a reaction. Insertion of Zn(II) into octaalkylporphyrins takes only seconds, although diarylporphyrins require longer. By omitting the base, insertion was complete in less than 3 h, and there was no evidence of acid cleavage of the Pt fragment, so addition of the base would appear to be unwarranted in future. In conclusion, the oxidative addition to form the free-base organoplatinum porphyrin followed by metallation is the favoured route for these first-row metal ions, and the C–Pt bond is robust enough to survive the metallations. This may not be true for more difficult metal ion insertions, such as those for second-row metals, but the alternative route via the DPPBr complexes should be appropriate.

In the interests of preparing more crowded organoplatinum porphyrins, we treated NiDPPBr_2 **18** with excess PtL_3. However, the maximum yield of bis Pt adduct {5,15-bis[*trans*-PtBr(PPh_3)$_2$](NiDPP)} **20** was 32%, after chromatographic separation from the intermediate mono-adduct {5-bromo-15-[*trans*-PtBr(PPh_3)$_2$](NiDPP)} **19**. We report here the crystal structure of **19**, but so far we have not obtained X-ray quality crystals of **20**. The latter was characterised both spectroscopically and electrochemically (see next section). We reported **19** previously as an intermediate in the synthesis of the unsymmetrical bis-metallo complex **21**, which possesses PdBr(PPh_3)$_2$ and PtBr(PPh_3)$_2$ moieties on opposite *meso* carbons.[9] The ability to achieve this selective two-step conversion is conferred by the strong deactivating effect of the $PtBrL_2$ substituent. We discuss this in more detail below.

Spectroscopy and electrochemistry

The ^{1}H and ^{31}P NMR spectra of the diamagnetic complexes are typical of this class of compound. As expected, the *trans*-bis(phosphine)Pt unit exhibits a singlet ^{31}P resonance with ^{195}Pt satellites, and ^1J(PtP) *ca.* 2950 Hz, a value typical for P *trans* to P. The substituent effect of the Pt fragment can be assessed by considering the chemical shifts of the porphyrin peripheral protons, most easily at the opposite *meso* position. In all cases, there is an upfield shift of this resonance with respect to the position for the precursor bromoporphyrin. The *meso*-proton chemical shifts for the bromoporphyrins are likewise upfield of those in the respective unsubstituted porphyrins. These shifts could be due to either or both of the following factors: (i) the group –PtBr(PPh_3)$_2$ is an electron donor; (ii) the bulky substituent causes out-of-plane distortions of the aromatic macrocycle, resulting in reduced ring current. The latter is certainly expected to apply, especially for the Ni(II) complexes (see X-ray section below). In all cases, there is also a red-shift of the electronic absorption bands upon substitution of the porphyrin by Br or the Pt fragment, and again this is probably due to a convolution of electronic effects on the porphyrin frontier π orbitals and non-planar distortions.

In order to assign the ^{1}H NMR spectrum of [PtBr(CoDPP)(PPh_3)$_2$] **14** we used comparisons with the precursors **8** and **5**. Porphyrin complexes of d^7 Co(II) give reasonably sharp ^{1}H resonances, exhibiting widths-at-half-heights of the *meso*

proton signal of *ca.* 200 Hz. The spectrum of CoDPP **5** is easily assigned by integration and linewidth considerations, as the lines narrow rapidly as the distance from the metal increases. The spectrum of **5** was reported for toluene solution by Shelnutt and co-workers,[17] and closely resembles our spectrum recorded in $CDCl_3$. The spectrum of **8** was more difficult to obtain because of the poor solubility, but the change of symmetry to C_{2v} was clear because of the split of the β-pyrrole signals into four lines. For the assignment of the *trans*-[PtBr(CoDPP)(PPh_3)$_2$] complex **14**, it only remained to locate the P-phenyl signals, and these were found as broad resonances at *ca* −2.2, 1.5 and 5.6 ppm. The isotropic shifts due to the unpaired electron in the d_{z^2} orbital of Co(II) are usually positive for protons near the plane of the porphyrin ring,[20] so these negative paramagnetically-induced shifts are to be expected for the protons of the phenyl rings on the PPh_3 ligands. In the diamagnetic *trans*-PtBr(PPh_3)$_2$ adducts, the *m*- and *p*-protons of the P-phenyl groups experience an upfield shift to the region of 6–6.5 ppm, because of the proportion of time they spend in the shielding zone of the magnetically anisotropic porphyrin ring. So for the Co(II) complex, this effect will be magnified by the upfield isotropic shift. The ^{31}P resonance for **14** is almost as sharp as those for the diamagnetic analogues, and occurs also at a very similar shift.

The situation for the chloro Mn(III) complexes, in which the metal ion is square-pyramidal d^4, with the $(d_{xy})^1(d_{yz})^1(d_{xy})^1(d_{z^2})^1$ configuration, is more complex. The spectrum of MnCl(DPP) **4**, prepared to assist in the assignments, could be interpreted by comparison with that of the analogous chloromanganese complex of *meso*-tetraphenylporphyrin (TPP).[21] The former exhibits upfield isotropic shifts of the β-pyrrole protons to *ca.* −25 ppm, and a large downfield shift of the *meso* proton to 45 ppm. The β-protons of MnCl(TPP) appear at −22.3 ppm.[21] The protons of the 5,15-phenyl groups of **4** appear as a broad unsymmetrical resonance peaking at *ca.* 8.4 ppm, and this apparently represents all three sets of phenyl protons. Why these do not split more clearly into *ortho*, *meta* and *para* sets is obscure, but again this is quite similar to what is found for the TPP analogue.[21] We could not obtain a spectrum of the bromoDPP complex **7** because of its low solubility. The signals for the Pt complex [PtBr(MnClDPP)(PPh_3)$_2$] (**13**) could be located by comparison with the spectrum of **4**, the β-pyrrole protons appearing in a 2:2:4 pattern at *ca.* −17, −22 and −31 ppm, and the *meso*-proton appeared as a very broad signal at *ca.* 47 ppm. The 10,20-phenyl group protons were observed in similar positions to those in **4**, and overlap a very broad unsymmetrical envelope spanning the region 3–15 ppm, which can only be due to the P-phenyl protons. One sharper signal protrudes at 7.0 ppm.

The ^{31}P spectrum of **13** is remarkably different from any of the others in the series. The spectrum is shown in Fig. 1, and one can see immediately the effects of the facial asymmetry of the square-pyramidal metalloporphyrin, apparently greatly amplified by the effects of the paramagnetism. The two ^{31}P resonances appear at 68 and −26 ppm, as a pair of doublets with a P–P coupling constant of *ca.* 420 Hz, a value consistent with a pair of non-equivalent *trans*-disposed phosphines. Interestingly, the average of these shifts is 21 ppm, placing it near the typical position for the complexes of Co, Ni and Zn. The signals are considerably broader than those for the other complexes, and the ^{195}Pt satellites appear as broad humps around the bases of the central lines. The two phosphines exchange environments by a rotation of the porphyrin *meso* carbon–platinum bond, so it is only the very large chemical shift difference brought about by the paramagnetism that enables us to see this separation. To investigate this point, ^{31}P spectra were recorded at temperatures up to 115 °C in $C_2D_2Cl_4$ solution, and although the two chemical shifts began to converge, it is clear that the coalescence temperature would be near 600 K. Attempts to investigate the solid-state structure of **13** were frustrated by the poor quality and twinning of the crystals, but the connectivity of the molecule was confirmed.

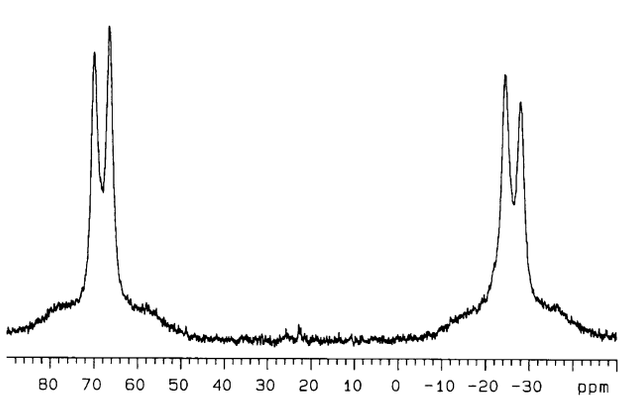

Fig. 1 31P NMR spectrum of *trans*-PtBr(MnClDPP)(PPh_3)$_2$ **13** in $CDCl_3$ at 293 K.

Table 2 Electrochemical data for peripherally-metallated porphyrins and precursors (in Bu_4NPF_6–CH_2Cl_2 *vs.* Ag/AgCl, 293 K)

Compound	E^0 (red1)/V	E^0 (ox1)/V
1	−1.05	+1.16
2	−0.93	+1.19
12	−1.32	+0.83
22	−1.24[a]	+0.89
6	−1.13	+1.17
9	−1.02	+1.20
16	−1.44	+0.90
20	−1.66	+0.61
23	−1.37[a]	+0.95

[a] Irreversible with loss of –PdBr(PPh_3)$_2$ moiety.

The effects of the Pt moiety on the redox properties of the porphyrin ring were studied for the free base and the nickel(II) complex by cyclic and ac voltammetry. For comparison, the unsubstituted DPP compounds **1** and **6** and the mono-bromo compounds **2** and **9** were also measured. The first reduction and oxidation potentials are summarized in Table 2. Experiments were conducted in CH_2Cl_2 with Bu_4NPF_6 as supporting electrolyte, and because of solubility constraints, the porphyrin concentrations were 7.5×10^{-4} M or less, which produced a relatively high background current. This meant that ac voltammetry generally gave better results than conventional cyclic voltammetry. The Pt-containing species gave good reversible or quasi-reversible waves, and the cyclic and ac voltammograms for [PtBr(H_2DPP)(PPh_3)$_2$] (**12**) are shown in Fig. 2. The voltammetric data, particularly the first oxidation potential,

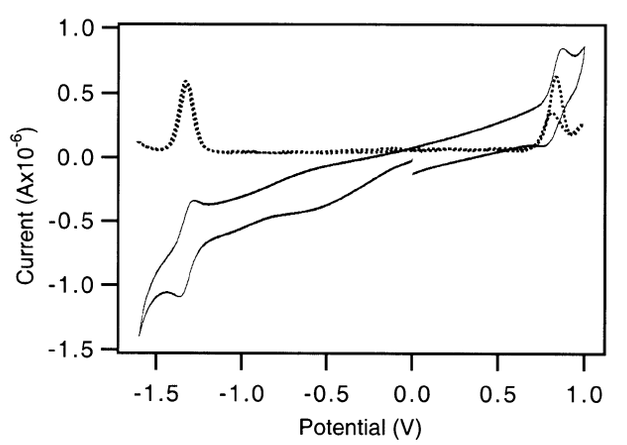

Fig. 2 Cyclic (200 mV s^{-1}, solid line) and ac (50 mV s^{-1}, dotted line) voltammograms of *trans*-PtBr(H_2DPP)(PPh_3)$_2$ **12** in CH_2Cl_2–Bu_4NPF_6 at 293 K.

Table 3 Selected geometric data (bond lengths, bond angles, phenyl group dihedral angles and displacements from macrocyclic mean planes) for *trans*-PtBr(MDPP)(PPh_3)$_2$ and *trans*-PtBr(NiDPPBr)(PPh_3)$_2$

	H_2DPP **12** (ref. 9)		CoDPP **14**		NiDPP **16**		ZnDPP **17**		
	mol. A	mol. B	mol. A	mol. B	mol. A	mol. B	mol. A	mol. B	NiDPPBr **19**
Bond lengths (Å)									
Pt–Br	2.518(1)	2.511(1)	2.527(2)	2.501(2)	2.504(3)	2.535(3)	2.521(2)	2.521(2)	2.517(1)
Pt–P1	2.323(3)	2.309(3)	2.367(4)	2.248(4)	2.232(7)	2.375(7)	2.302(5)	2.327(5)	2.329(2)
Pt–P2	2.307(3)	2.325(3)	2.268(4)	2.374(4)	2.389(7)	2.264(7)	2.328(5)	2.316(5)	2.305(2)
Pt–C5	2.05(1)	1.95(1)	1.95(1)	2.06(2)	2.02(2)	1.97(2)	1.98(2)	2.02(2)	2.011(5)
M–N1			1.96(1)	1.94(1)	1.94(2)	1.99(2)	2.04(2)	2.03(2)	1.930(4)
M–N2			1.97(1)	1.94(1)	1.91(2)	1.96(2)	2.00(2)	2.05(2)	1.919(4)
M–N3			1.97(1)	1.97(1)	1.96(2)	1.93(2)	2.06(2)	2.05(2)	1.939(5)
M–N4			1.95(1)	1.96(1)	1.94(2)	1.93(2)	2.02(2)	2.04(2)	1.933(5)
Bond angles (°)									
Br–Pt–P1	89.52(8)	91.80(9)	90.2(1)	91.4(1)	92.7(2)	89.3(2)	91.3(1)	90.4(1)	89.38(6)
Br–Pt–P2	88.88(8)	91.12(9)	89.3(1)	90.2(1)	89.7(2)	89.3(2)	89.9(1)	89.7(1)	91.32(6)
Br–Pt–C5	175.0(3)	177.2(3)	178.1(5)	175.9(4)	176.6(7)	177.5(7)	177.9(5)	178.0(5)	177.6(2)
P1–Pt–P2	176.2(1)	176.8(1)	177.5(2)	178.1(2)	177.4(2)	178.3(2)	178.4(2)	179.1(2)	176.2(6)
P1–Pt–C5	92.6(3)	89.9(3)	90.1(5)	92.7(4)	90.7(7)	89.0(7)	90.2(5)	91.6(5)	88.4(2)
P2–Pt–C5	89.2(3)	87.3(3)	90.4(5)	85.7(4)	86.9(7)	92.4(7)	88.5(5)	88.4(5)	90.9(2)
Pt–C5–C4	116.2(8)	121.7(8)	119(1)	122(1)	121(2)	119(2)	117(1)	120(2)	119.0(4)
Pt–C5–C6	118.3(8)	118.4(8)	122(1)	120(1)	123(2)	123(2)	123(1)	116(2)	120.6(4)
Dihedral angles of the 10,20 phenyl substituents to the macrocyclic mean plane (°)									
10–Ph	56.8	66.3	128.5	113.8	129.3	113.9	126.4	113.5	50.2
20–Ph	71.2	93.2	79.9	114.5	79.5	113.1	80.2	114.9	81.7
Distances of selected atoms from the macrocyclic mean plane (Å)									
C5	+0.13	−0.10	−0.17	+0.08	−0.28	+0.14	−0.16	+0.03	+0.31
C10	−0.11	+0.03	+0.32	−0.19	+0.30	−0.22	+0.21	−0.18	−0.46
C15	+0.05	−0.06	−0.30	+0.13	−0.40	+0.19	−0.24	+0.06	+0.48
C20	−0.07	+0.04	+0.29	−0.10	+0.32	−0.10	+0.24	−0.07	−0.46
M			+0.03	+0.02	−0.05	−0.03	+0.01	−0.04	−0.01
Pt	+0.19	−0.52	−0.11	+0.07	−0.31	−0.06	−0.15	−0.02	+0.37
Br	+0.20	−1.13	−0.03	−0.12	−0.20	−0.23	−0.06	−0.16	+0.34

clearly confirm the proposal that the –Pt(PPh_3)$_2$Br group is a strong electron donor. This is manifest in a cathodic shift of about 300 mV, for both the free base **12** and the corresponding Ni(II) complex **16**. Moreover, the effect of a second Pt substituent is essentially additive, and the first oxidation potential of {5,15-bis[*trans*-PtBr(PPh_3)$_2$](NiDPP)} **20** is remarkably low for a Ni(II) porphyrin, namely +0.61 V (Fc/Fc^+ at +0.55 V) . The fact that both the free base and the Ni(II) complexes exhibit very similar effects is good evidence that (i) oxidation occurs at the porphyrin ring, not at the Ni(II) centre and (ii) the changes in spectra and electrode potentials due to the Pt substituent are electronic in origin, and not related to out-of-plane distortions in the Ni(II) complexes. Similar effects are noted for the corresponding compounds **22** and **23** containing the *palladium* bis(phosphine) fragment, although the shifts in redox potentials are not quite as large (Table 2), and the first reduction is irreversible, with loss of the Pd substituent. Literature searching reveals no comparable electrochemical data for simple aryls, *e.g.* phenyl-platinum(II) or -palladium(II) organometallics, but there have been several studies of the substituent effects of nickel(II), palladium(II) and platinum(II) on aromatic rings using ^{1}H, ^{19}F or ^{13}C NMR data.[23,24] The last piece of evidence for a strong electron-donating substituent effect is the remarkable decrease in reactivity towards the second oxidative addition in the attempted conversion of $NiDPPBr_2$ to **20**. Clearly the Pt substituent is decreasing the polarity of the opposite C–Br bond and inhibiting the insertion of the Pt(0) moiety. Stang and co-workers noted in their work on double Pt(PPh_3)$_2$ addition to 4,4′-diiodobiphenyl, a similar but apparently weaker electron-donating effect.[23]

Crystal structures

An objective of this work was to compare the coordination chemistry of late first-row transition metal ions with the new organoplatinum porphyrin ligands and to study the structures of both the ligands and complexes by single-crystal X-ray crystallography wherever possible. We have previously reported the structure of *trans*-[PtBr(H_2DPP)(PPh_3)$_2$].[9] In this present study, we have extended the structural analysis of this system, completing structure determinations for *trans*-[PtBr(MDPP)-(PPh_3)$_2$]·0.5CH_2Cl_2 for M = Ni (**16**), Co (**14**) and Zn (**17**), and *trans*-[PtBr(NiDPPBr)(PPh_3)$_2$] **19**, the preparation and spectroscopic characterisation of **16** having been reported previously.[9]

***trans*-[PtBr(NiDPPBr)(PPh_3)$_2$] (19).** This complex crystallizes in the triclinic space group $P\bar{1}$ with one molecule comprising the asymmetric unit. A representative view of the structure of the molecule is shown in Fig. 3. Relevant geometric parameters are listed in Table 3. The *trans* PPh_3 ligands adopt threefold propeller conformations of opposite chirality and are

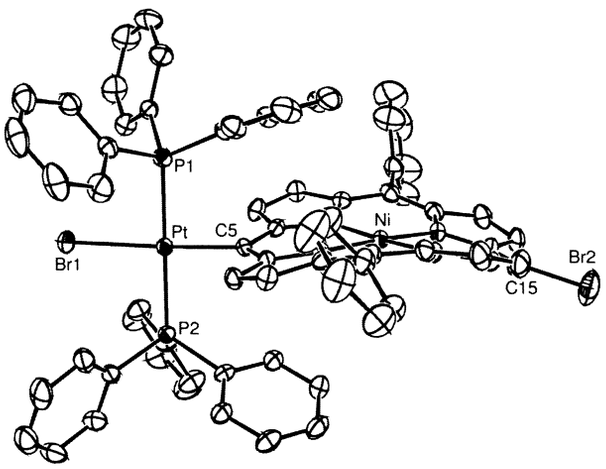

Fig. 3 Molecular structure of *trans*-PtBr(NiDPPBr)$(PPh_3)_2$ **19** (hydrogen atoms omitted for clarity).

related by a pseudo-mirror plane of symmetry. Ring 1 on each ligand overhangs the porphyrin macrocycle in face-to-face contact with the second pyrrole ring. The porphyrin ring is symmetrically coordinated to the platinum through the C5 *meso* carbon with Pt–C5–C(4,6) angles of 120.6(4) and 119.0(4)°, respectively. The coordination geometry about the platinum atom (Table 3) is very similar to that found in the analogous H_2DPP complex,[9] showing that insertion of metal atoms into the macrocyclic ring and substitution of a bromine atom at C15 exerts only minimal influence on this geometry.

The coordinated nickel lies in the macrocyclic mean plane ($C_{20}N_4$) and adopts the expected square planar geometry with Ni–N bond lengths ranging from 1.919(4)–1.939(5) Å. The porphyrin macrocycle is not flat, but rather adopts a distorted shape with C10 and C20 respectively 0.46, 0.45 Å below and C5 and C15 respectively 0.31, 0.48 Å above the macrocyclic plane (see below). The Pt atom and its coordinated Br atom lie respectively 0.37 and 0.34 Å above this plane while the bromine bonded to C15 lies 1.03 Å above the plane. The substituent phenyl groups at C10 and C20 are twisted by 31.5° with respect to each other and lie at dihedral angles of 81.7 and 50.2° to the macrocyclic mean plane.

***trans*-[PtBr(MDPP)$(PPh_3)_2$]·0.5CH_2Cl_2, M = Co (14), Ni (16), Zn (17).** The structures of these three compounds are isomorphous, crystallizing in space group $P2_1$ with a ~13.4, b ~ 29.7, c ~ 14.4 Å, and β ~ 91°. The asymmetric unit consists of two independent molecules of the complex with a co-crystallized molecule of dichloromethane (modelled with 50% occupancy) located in the vicinity of the PPh_3 phenyl substituents. As a representative of the set, the molecules of the cobalt complex **14** are shown in Fig. 4. Relevant geometric parameters are listed in Table 3. The conformational structures of the two molecules are very similar with the exception of the relative orientations of the phenyl substituents on C10 and C20 of the porphyrin ring. For molecule A, these two rings are twisted by approximately 45° with respect to other while for molecule B, the two rings are essentially parallel. As for the other *trans* complexes in this series, the PPh_3 ligands adopt three-fold propeller conformations and are related by a pseudo-mirror plane of symmetry with ring 1 on each ligand overhanging the macrocycle in face-to-face contact with the second pyrrole ring. The coordination geometry about the platinum atom shows a considerable dispersion of values across the three complexes with Pt–Br in the range 2.501(2)–2.535(3) Å with an average value of 2.51(1) Å, Pt–P in the range 2.264(4)–2.389(7) Å with an average value of 2.32(5) Å and Pt–C in the range 1.95(1)–2.06(2) with an average value of. 2.00(4) Å. These average values are consistent with those observed for the other members of the

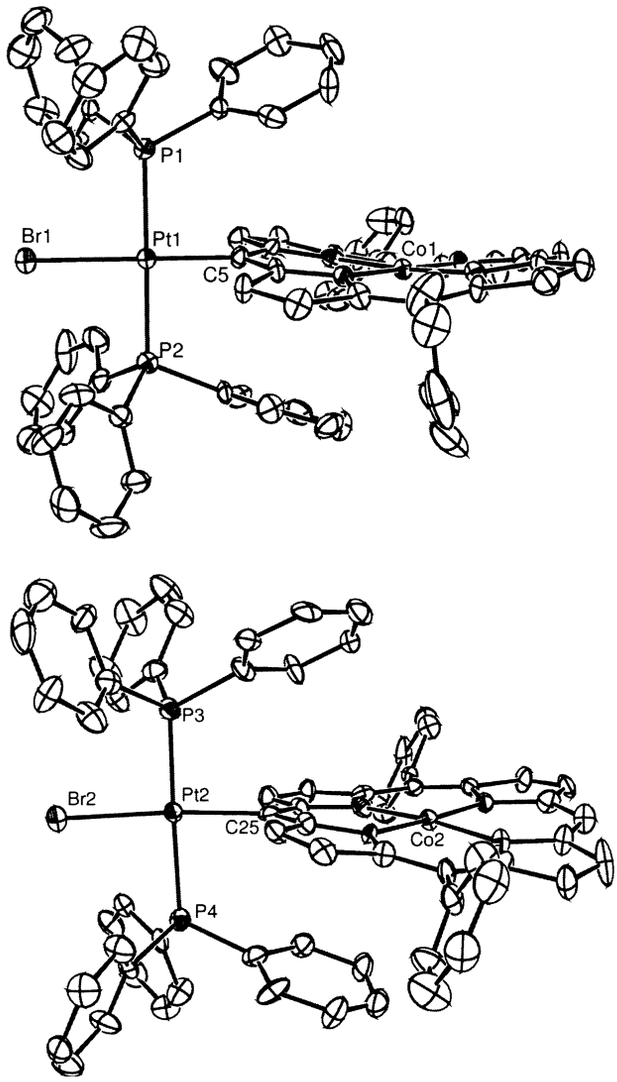

Fig. 4 Molecular structure of *trans*-PtBr(CoDPP)$(PPh_3)_2$ **14** (hydrogen atoms omitted for clarity; molecule 1, top; molecule 2, bottom).

series and correlation effects between the two molecules may be the cause of the observed range of values.

Non-planar distortions of the porphyrin rings

Given the novelty of our –$PtBrL_2$ substituent, and the fact that we now have crystal structures for the free base and several metallo derivatives, it is worthwhile to examine the steric consequences of platinum attachment on the planarity of the porphyrin macrocycle. As is common for many Ni(II) porphyrin structures,[17,24,25] the porphyrin ring in complexes **16** and **19** is not planar, but rather adopts a distorted shape due to the short Ni–N bond distances (average of all over the two complexes 1.94 Å). The details of the non-planar distortions for **19** are displayed in linear form in Fig. 5 as the vertical displacement of the atom from the $C_{20}N_4$ plane. Similar plots for the complexes **14**, **16** and **17** as well as the free base **12**[9] are provided in the ESI.† The metal–nitrogen bond distances are quite typical for these divalent four-coordinate metals in porphyrin complexes, resulting in the order Zn–N > Co–N > Ni–N. This order is reflected in the typical pattern of out-of-plane distortions (Zn < Co < Ni) in response to the contraction of the MN_4 core.[25] The most typical distorted conformations for four-coordinate metalloporphyrins are "ruffled" and "saddled". In the former, the *meso* carbons are alternately up and down with respect to the macrocycle plane, while in the latter, it is the pairs of pyrrole β carbons which lie alternately out of the plane. In our structures, the free base is virtually planar, but the four metallo

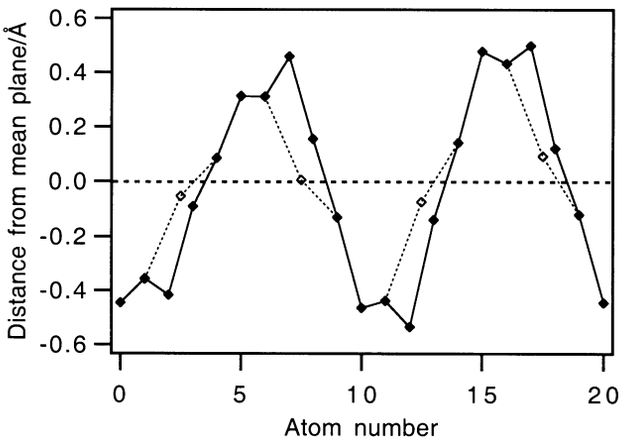

Fig. 5 Linear display of the deviations of the macrocycle atoms from the $C_{20}N_4$ least-squares plane for the complex *trans*-PtBr(NiDPPBr)$(PPh_3)_2$ **19** (solid diamonds are carbons, open diamonds are nitrogens).

derivatives adopt an interesting hybrid of the ruffled and saddled conformations. As can be seen in Fig. 5, this results in both the *meso* carbon and the next two carbons of the pyrrole ring being the farthest out of the plane (*e.g.* see carbons 5, 6 and 7). Thus the pyrrole rings are tilted as in a typical ruffled structure, but the axes of the major out-of-plane displacement are rotated to lie between normal ruffling and saddling axes. This pattern applies consistently to all four of our structures, and results in the atoms 2, 7, 12 and 17 having the largest displacements from the plane in all but one case out of the nine molecules (C20 in **19**).

Conclusion

The ease of preparation of these platinio-porphyrins and their chemical robustness makes them promising candidates as porphyrin building blocks from which supramolecular arrays may be derived. The fact that the phosphine ligands, the lateral aryl groups on the porphyrin, and the centrally-coordinated metal ion can all be varied, allows the synthesis of a wide variety of structures. The strong electron-donating influence of the $–PtBrL_2$ unit may be useful in tailoring the properties of porphyrins. This moiety provides an inert substituent which causes a strong cathodic shift of the redox potentials. However, the lowered oxidation potentials may force us to rethink our original proposal that the phosphine ligand superstructure could provide selective cavities for biomimetic metalloporphyrin-catalysed oxidations. Experiments to investigate this point, and to use the Pt substituents as scaffolds for multiporphyrin supramolecules are planned for the near future.

Acknowledgements

We thank the Australian Research council for a Small Grant to D. P. A. and for financial support for the purchase of the diffractometer, and the Faculty of Science, Q.U.T. for a postgraduate scholarship for M. J. H. D. P. A. thanks Prof. J. Jiang (Shandong University, Jinan, China) and the Research School of Chemistry, The Australian National University, for Visiting Fellowships. We also thank Dr Alison Edwards, Research School of Chemistry, The Australian National University, for the confirmatory structure determination of **13**.

References

1 (*a*) P. J. Brothers, *Adv. Organomet. Chem.*, 2001, **46**, 223; (*b*) R. Guilard, A. Tabard, E. van Caemelbecke and K. M. Kadish, in *The Porphyrin Handbook*, ed. K. M. Kadish, K. M. Smith and R. Guilard, Academic Press, San Diego, CA, 2000, vol. 3, ch. 21, pp. 295–345.
2 N. J. Gogan and Z. U. Siddiqui, *Can. J. Chem.*, 1972, **50**, 720.
3 (*a*) K. K. Dailey, G. P. A. Yap, A. L. Rheingold and T. B. Rauchfuss, *Angew. Chem., Int. Ed. Engl.*, 1996, **35**, 1833; (*b*) K. K. Dailey and T. B. Rauchfuss, *Polyhedron*, 1997, **16**, 3129.
4 S. M. Contakes, S. T. Beatty, K. K. Dailey, T. B. Rauchfuss and D. Fenske, *Organometallics*, 2000, **19**, 4767.
5 (*a*) See, for example: H. Furuta, T. Ogawa, Y. Uwatoko and K. Araki, *Inorg. Chem.*, 1999, **38**, 2676; (*b*) P. J. Chmielewski and L. Latos-Grazynski, *Inorg. Chem.*, 1997, **36**, 840; (*c*) P. J. Chmielewski, L. Latos-Grazynski and I. Schmidt, *Inorg. Chem.*, 2000, **39**, 5475; (*d*) K. Araki, H. Winnischofer, H. J. Toma, H. Maeda, A. Osuka and H. Furuta, *Inorg. Chem.*, 2001, **40**, 2020; (*e*) I. Schmidt and P. J. Chmielewski, *Chem. Commun.*, 2002, 92.
6 S. R. Graham, G. M. Ferrence and T. D. Lash, *Chem. Commun.*, 2002, 894.
7 D. P. Arnold, R. C. Bott, H. Eldridge, F. Elms, G. Smith and M. Zojaji, *Aust. J. Chem.*, 1997, **50**, 495.
8 D. P. Arnold, Y. Sakata, K. Sugiura and E. I. Worthington, *Chem. Commun.*, 1998, 2331.
9 D. P. Arnold, P. C. Healy, M. J. Hodgson and M. L. Williams, *J. Organomet. Chem.*, 2000, **607**, 41.
10 A. G. Hyslop, M. A. Kellett, P. M. Iovine and M. J. Therien, *J. Am. Chem. Soc.*, 1998, **120**, 12676.
11 (*a*) K. M. Smith, G. H. Barnett, B. Evans and Z. Martynenko, *J. Am. Chem. Soc.*, 1979, **101**, 5953; (*b*) H. J. Shine, G. A. Padilla and S.-M. Wu, *J. Org. Chem.*, 1979, **44**, 4069.
12 L. Ruhlmann and A. Giraudeau, *Eur. J. Inorg. Chem.*, 2001, 659.
13 K. M. Smith, K. C. Langry and O. M. Minnetian, *J. Org. Chem.*, 1984, **49**, 4602.
14 S. G. DiMagno, V. S.-Y. Lin and M. J. Therien, *J. Org. Chem.*, 1993, **58**, 5983.
15 S. Shanmugathasan, C. K. Johnson, C. Edwards, E. K. Matthews, D. Dolphin and R. W. Boyle, *J. Porphyrins Phthalocyanines*, 2000, **4**, 228.
16 R. Ugo, F. Cariati and G. La Monica, *Inorg. Synth.*, 1990, **28**, 123.
17 X.-Z. Song, L. Jaquinod, W. Jentzen, D. J. Nurco, S.-L. Jia, R. G. Khoury, J.-G. Ma, C. J. Medforth, K. M. Smith and J. A. Shelnutt, *Inorg. Chem.*, 1998, **37**, 2009.
18 Molecular Structure Corporation (1997–2001). teXsan for Windows. Version 1.06. MSC, 9009 New Trails Drive, The Woodlands, TX, 77831, USA.
19 V. V. Borovkov, J. M. Lintuluoto and Y. Inoue, *Synlett*, 1999, 61.
20 G. N. La Mar and F. A. Walker, *J. Am. Chem. Soc.*, 1973, **95**, 1790.
21 (*a*) G. N. La Mar and F. A. Walker, *J. Am. Chem. Soc.*, 1975, **97**, 5103; (*b*) P. Turner and M. J. Gunter, *Inorg. Chem.*, 1994, **33**, 1406.
22 (*a*) G. W. Parshall, *J. Am. Chem. Soc.*, 1974, **96**, 2360; (*b*) H. C. Clark and J. E. H. Ward, *J. Am. Chem. Soc.*, 1974, **96**, 1741; (*c*) D. R. Coulson, *J. Am. Chem. Soc.*, 1976, **98**, 3111.
23 J. Manna, C. J. Kuehl, J. A. Whiteford and P. J. Stang, *Organometallics*, 1997, **16**, 1897.
24 J. A. Shelnutt, X.-Z. Song, J.-G. Ma, S.-L. Jia, W. Jentzen and C. J. Medforth, *Chem. Soc. Rev.*, 1998, **27**, 31.
25 W. R. Scheidt, in *The Porphyrin Handbook*, ed. K. M. Kadish, K. M. Smith and R. Guilard, Academic Press, San Diego, CA, 2000, vol. 3, ch. 16, pp. 49–112.